SOFT SWITCHING AC/DC/AC CONVERTER WITH CURRENT FREEWHEELING CIRCUIT

Byeong O. Woo and Gyu H. Cho

Dept. of Electrical Engineering,
Korea Advanced Institute of Science and Technology (KAIST)
P.O.Box 150 Chongryang, Seoul 130-650, Korea
(FAX.: 82-2-960-2103)

ABSTRACT

The Modified DC-Link(MDCL) converter generating sinusoidal output voltage solved the drawbacks of recently developed soft switching converters such as high voltage stresses of devices and/or many device counts[1]. However, it also has problems such as the high peak device current and a wide variation of switching cycle interval.

In this paper newly improved soft switching ac/dc/ac converter based on high frequency link is proposed to solve these problems. By introducing a current freewheeling circuit, it separates the main power flow from the resonating circuit during commutation interval. As a result, the peak current is limited to around link current and switching cycle interval is controllable. Furthermore, the VA ratings of the devices is considerably reduced. Therefore, this converter combines the desired features of the MDCL converter with its improvements.

I. INTRODUCTION

A number of converter topologies have been investigated to achieve soft switching in high power converter where soft switching enables the converter to operate at higher switching frequency by reducing the switching losses[1]-[9]. Soft switching circuit topologies can be classified into two; resonant link schemes attaining soft switching condition by the resonant action of the link and resonant pole schemes attaining it by the operation of each pole. These converter topologies have many advantages such as high performance, high power density and high efficiency etc.

The resonant dc-link and active clamped resonant dc-link inverter have been well established and known to be successful ones[2][3], however, the inverter switching should be synchronized to resonating link for zero-voltage switching. A higher switching frequency is required to obtain the same performance as a conventional PWM inverter because of discrete pulse modulation. Several literatures have been reported to realize true pulse width modulation capability in the resonant link converter. Since these converters employ resonant circuit to the link, it has imposed a penalty with respect to device voltage stress.

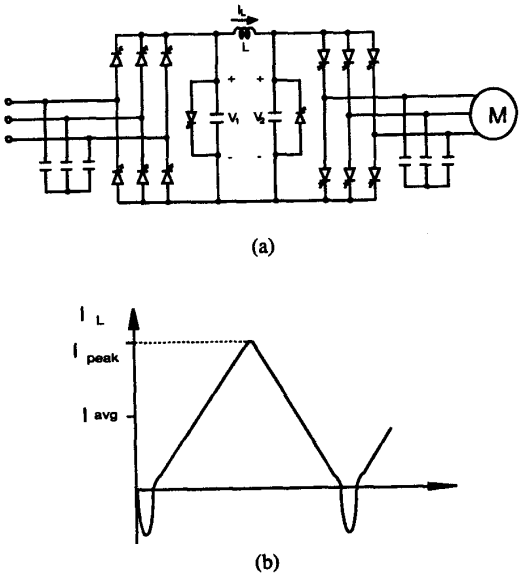

Fig. 1 (a) Modified DC-Link converter
(b) Link current waveform of MDCL converter

The shortcomings of soft switching converters to date are such that resonant link schemes typically impose large voltage stresses on switching devices and resonant pole schemes either impose twice current rating or require twice device count compared to the hard switched inverter.

The Modified DC-Link(MDCL) converter as shown in Fig. 1 was proposed at which the voltage stresses of switching devices did not exceed more than

0-7803-0090-4/91/0700-0031$01.00 ©1991IEEE

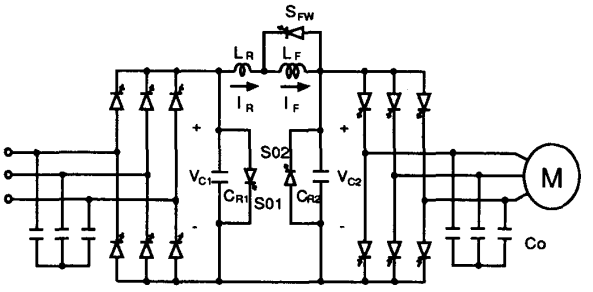

Fig. 2 Proposed converter configuration

10% of the maximum line-to-line source voltage and only two additional switches were needed to realize ac/dc/ac converter[1]. Unfortunately, the peak current of link inductor in MDCL converter reaches several times average link current so that the current ratings of switching devices are increased and every switching cycle interval widely varies according to the inverter input side voltage.

In this paper a new converter with current freewheeling circuits is proposed to solve the aforementioned drawbacks of MDCL converter. The introduction of a current freewheeling circuit makes it possible to separate the main power flow from the resonating circuit during commutation interval. As a result, the device current is limited to around the average link current and the switching cycle interval is controllable. Therefore, this converter combines the desired features of the MDCL converter with its improvements.

II. DESCRIPTION OF PROPOSED CONVERTER

The proposed converter configuration is shown in Fig. 2 which consists of a front-end converter, modified dc-link including current freewheeling circuit, inverter and output filter capacitors. The front-end converter is controlled for its output voltage to be among V_S, $-V_S$ and zero where V_S represents the maximum line-to-line source voltage neglecting the ripple. Two shunt capacitors of the modified dc-link provide zero voltage switching conditions for the front-end converter and the inverter, respectively. The switch S_{FW} commutated at zero-current condition provides the freewheeling path of the link current during the commutation interval. By doing so, the commutation operation is separated from the main power flow. Inverter full bridge composed of six switches impresses the link current cycle by cycle to the proper output filter capacitor so that the output voltage follows the sinusoidal reference value.

For the simplicity of explanation it is assumed that
1) output filter capacitor C_O is much larger than C_R to be approximated by a voltage source during commutation interval ($C_O \gg C_{R1} = C_{R2}$),
2) inductor L_F is much larger than L_R to be approximated by a current source ($L_F \gg L_R$),
3) the switching time of the switches is zero,
4) the voltage drop across the conducting devices is negligible.

III. OPERATION AND ANALYSES

The operation modes of this converter are directly dependent on the polarity of the reflected voltage from the filter capacitor to the link during the conduction period of selected inverter switches and it is divided into powering and regenerative ones. Since the main current on the link flows from the input side to the output side, the power flow is determined by the link voltage. The input side link voltage $v_{C1}(t)$ and the output side link voltage $v_{C2}(t)$ are zero and/or positive during powering operation and they are zero and/or negative during regenerative one. Therefore the direction of power flow is positive(negative) during powering(regenerative) operation.

Fig. 3 shows the eight modes of powering operation. Assume that the current of inductor L_F is $I_F(k)$ and freewheels through S_{FW} and capacitor C_{R2} is charged to αV_S ($\alpha \geq 1$) while the current of inductor L_R and capacitor voltage $v_{C1}(t)$ are zero. And all switches except S_{FW} are turned-off.

1) **Mode P1** : Since the inductor current I_f is freewheeling through S_{FW}, the capacitor voltage $v_{C2}(t)$ starts to resonate in series with S_{FW}, L_R and, C_{R1}. After $v_{C1}(t)$ reaches its peak αV_S, it starts to decrease. In this interval the inductor currents and the capacitor voltages are given by

$$i_{Lr}(t) = -\frac{v_{C2}(t_0)}{2Z_r}\sin\sqrt{2}\omega_r t \tag{1.1}$$

$$i_{Lf}(t) = I_F(t) \tag{1.2}$$

$$v_{C1}(t) = \frac{v_{C2}(t_0)}{2}(1-\cos\sqrt{2}\omega_r t) \tag{1.3}$$

$$v_{C2}(t) = \frac{v_{C2}(t_0)}{2}(\cos\sqrt{2}\omega_r t - 1) + v_{C2}(t_0) \tag{1.4}$$

where $Z_r = \sqrt{L_R/C_R}$, $\omega_r = 1/\sqrt{L_R C_R}$ and $v_{C2}(t_0) = \alpha V_S$.
This mode ends when $v_{C1}(t)$ is decreased to be V_S.

2) **Mode P2** : When $v_{C1}(t)$ reaches V_S the selected switch pair of the front-end converter are turned-on under the zero-voltage switching condition. During this interval

$$i_{Lr}(t) = I_2\sin\omega_r t + i_{Lr}(t_1)\cos\omega_r t \tag{2.1}$$

$$i_{Lf}(t) = I_F(k) \tag{2.2}$$

$$v_{C1}(t) = V_S \tag{2.3}$$

$$v_{C2}(t) = \frac{1}{C_R\omega_r}(i_{Lr}(t_1)\sin\omega_r t - I_2\cos\omega_r t) + V_S \tag{2.4}$$

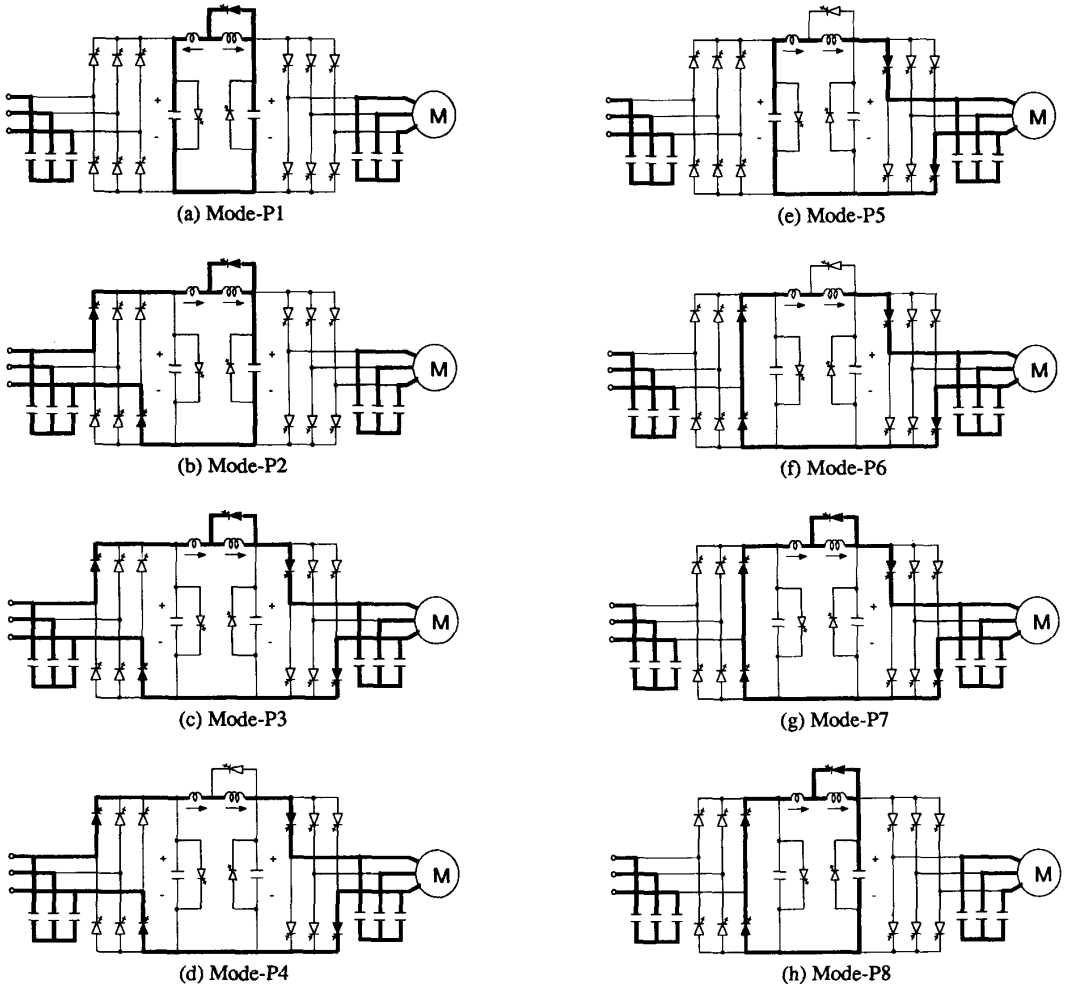

(a) Mode-P1 (e) Mode-P5

(b) Mode-P2 (f) Mode-P6

(c) Mode-P3 (g) Mode-P7

(d) Mode-P4 (h) Mode-P8

Fig. 3 Mode diagrams of powering operation

where $I_2 = \dfrac{V_S - v_{C2}(t_1)}{Z_r}$.

3) **Mode P3** : On reaching $v_{C2}(t)$ to V_I, the inverter switches start to conduct. $i_{Lr}(t)$ is increased while $i_{Lf}(t)$ freewheels through S_{FW}. Neglecting the voltage variation of the output capacitor in this interval, the equations are given by

$$i_{Lr}(t) = \frac{1}{L_R}(V_S - V_I)t + i_{Lr}(t_2) \tag{3.1}$$

$$i_{Lf}(t) = I_F \tag{3.2}$$

$$v_{C1}(t) = V_S \tag{3.3}$$

$$v_{C2}(t) = V_I . \tag{3.4}$$

4) **Mode P4** : When $i_{Lr}(t)$ becomes $I_F(k)$, S_{FW} is turned off at zero-current switching conduction. The link current is almost linearly increased. Thus

$$i_{Lr}(t) = i_{Lf}(t) = \frac{1}{L_R + L_F}(V_S - V_I)t + I_F(k) \tag{4.1}$$

$$v_{C1}(t) = V_S \tag{4.2}$$

$$v_{C2}(t) = V_I . \tag{4.3}$$

When the link current reaches the wanted value, $I_F(k) + \Delta I_F$ this mode ends by turning-off the front-end converter switches.

5) **Mode P5** : The capacitor C_R is almost linearly discharged. Since this interval is short enought to neglect the inductor current variation. During this interval

$$i_{Lr}(t) = i_{Lf}(t) \approx I_F(k) + \Delta I_F \tag{5.1}$$

$$v_{C1}(t) = V_S - \frac{I_F(k) + \Delta I_F}{C_R}t \tag{5.2}$$

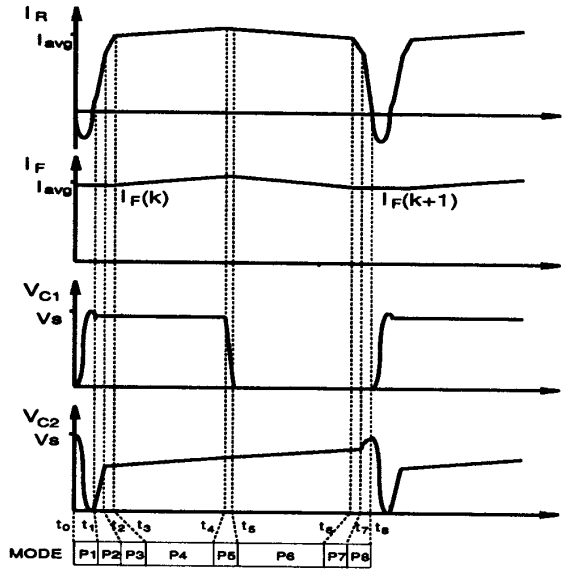

Fig. 4 Typical voltage and current waveforms during powering operation

$$v_{C2}(t) = V_I \,. \tag{5.3}$$

6) **Mode P6** : One leg of the front-end converter conducts when $v_{C1}(t)$ becomes zero. During this mode the link current is decreased.

$$i_{Lr}(t) = i_{Lf}(t) = I_F(k) + \Delta I_F - \frac{1}{L_R + L_F} V_I t \tag{6.1}$$

$$v_{C1}(t) = 0 \tag{6.2}$$

$$v_{C2}(t) = V_I \tag{6.3}$$

This mode ends when $i_{Lr}(t)$ is decreased to the wanted value $I_F(k+1)$ that is the freewheeling current during next commutation interval.

7) **Mode P7** : Switch S_{FW} is gated on so that the link current freewheels through it, The current $i_{Lr}(t)$ decays abruptly since V_I is applied to L_R. The equations are given by

$$i_{Lr}(t) = I_F(k+1) - \frac{1}{L_R} V_I t \tag{7.1}$$

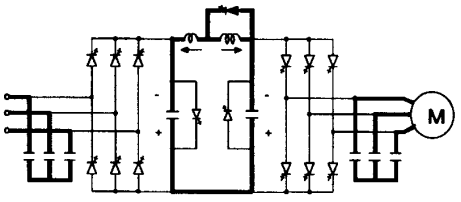

(a) Mode-R1

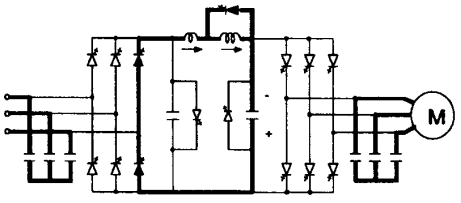

(b) Mode-R2

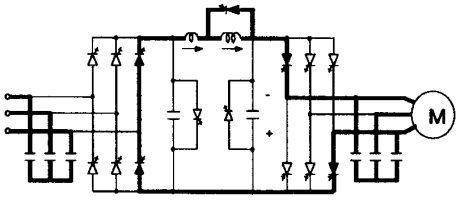

(c) Mode-R3

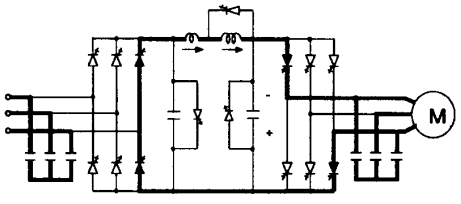

(d) Mode-R4

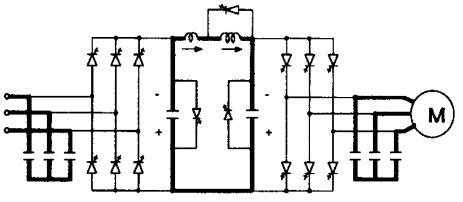

(e) Mode-R5

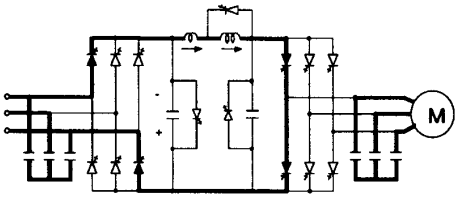

(f) Mode-R6

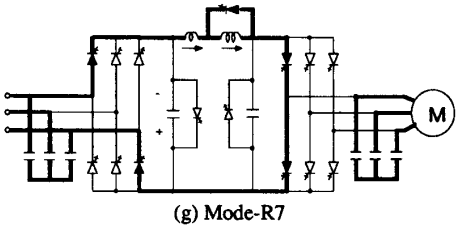

(g) Mode-R7

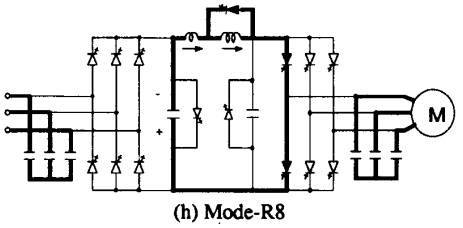

(h) Mode-R8

Fig. 5 Mode diagrams of regenerative operation

$$i_{Lf}(t) = I_F(k+1) \tag{7.2}$$

$$v_{C1}(t) = 0 \tag{7.3}$$

$$v_{C2}(t) = V_I \tag{7.4}$$

This mode ends when $i_{Lr}(t)$ is decreased to be I_{COM} which is defined as :

$$I_{COM} = \frac{1}{Z_r}\sqrt{(\alpha V_S)^2 - V_I^2} \tag{7.5}$$

where $Z_r = \sqrt{L_R / C_R}$.

8) **Mode P8** : Inductor current i_{Lf}(t) continues to freewheel and the trapped energy to inductor L_R is transferred to the inverter side shunt capacitor by resonance :

$$i_{Lr}(t) = I_8 \sin\omega_r t + i_{Lr}(t_7)\cos\omega_r t \tag{8.1}$$

$$i_{Lf}(t) = I_F(k+1) \tag{8.2}$$

$$v_{C1}(t) = 0 \tag{8.3}$$

$$v_{C2}(t) = \frac{1}{C_R \omega_r}(i_{Lr}(t_7)\sin\omega_r t - I_8 \cos\omega_r t) + v_{C2}(t_7) - V_I \tag{8.4}$$

where

$$I_8 = \frac{-V_I}{Z_r}.$$

When $i_{Lr}(t)$ becomes zero at $t = t_8$, voltage $v_{C2}(t)$ reaches its peak value. From the energy conservation and equation (7.4) and (7.5), the peak value is given by

$$v_{C2}(t_8) = \sqrt{v_{C2}(t_7)^2 + (L_R / C_R)\, i_{Lr}(t_7)^2} = \alpha V_S. \tag{8.5}$$

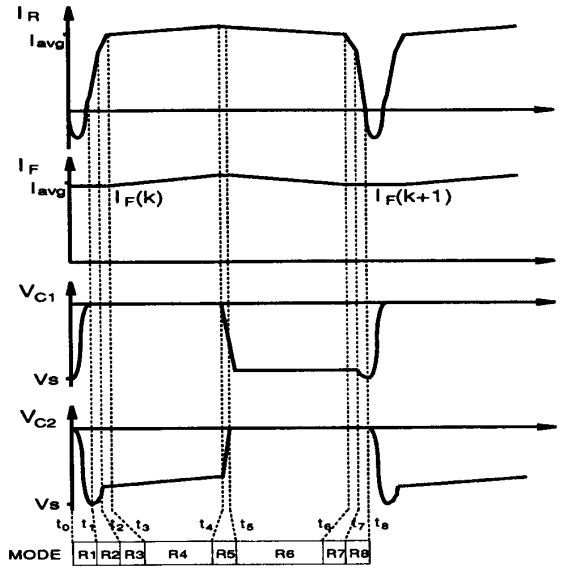

Fig. 6 Typical voltage and current waveforms during regenerative operation

All states are the same as those of the beginning of Mode P1, therefore, one switching cycle is completed.

Fig. 4 shows the current and voltage waveforms of the proposed converter operating on the powering modes. The regenerative operation is similar to the powering operation and consists of eight modes as shown in Fig. 5. The typical current and voltage waveforms during regenerative operation is shown in Fig. 6. However unlike the powering operation the reflected voltage V_I is negative and the front-end converter switches are selected in such a manner that the output voltage of the front-end converter becomes the minimum line-to-line source voltage.

IV. CONTROL STRATEGY AND CHARACTERISTICS

Basically this converter operates to generate sinusoidal output voltage independently to the load condition. Since the main current flow on the link is always positive direction from the front-end converter side to the inverter side, turning-on the upper switch of an inverter leg causes the corresponding phase voltage to increase, on the other hand turning-on the lower switch of a leg causes the phase voltage to decrease. By gating-on the proper switches of inverter bridge, the maximum error phase of which error between the reference voltage and the actual phase voltage is the largest among three phases is compensated every switching cycle. Fig. 7 shows the diagram for mode transition between powering modes and regenerative modes. In this converter transition between powering operation and regenerative operation is easily accomplished by turning on S01 or S02. Consequently it is possible to conduct any inverter switch pair in each switching cycle and to supply current to the selected output terminal so that the voltage of output capacitors can be controlled to follow the sinusoidal references.

For the powering operation the link current $i_{Lf}(t)$ freewheels during commutation interval (Δt_1, Δt_2, Δt_3, Δt_7, and Δt_8) and the capacitor charging interval (Δt_5) is short enough to neglect the current variation during this interval, therefore, the link current is actually changed during Δt_4 and Δt_6 as shown in Fig. 8. The link current is given by

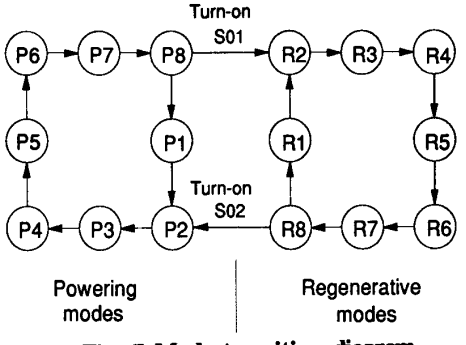

Fig. 7 Mode transition diagram

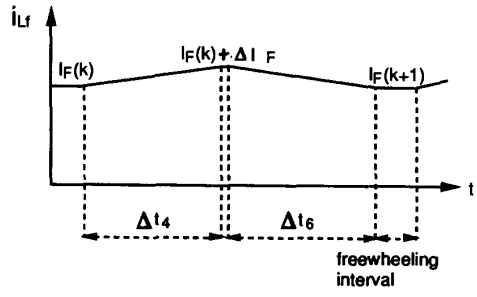

Fig. 8 Link current control

$$I_F(k+1)=I_F(k)+\frac{V_S-V_I}{L_R+L_F}\Delta t_4 - \frac{V_I}{L_R+L_F}\Delta t_6 \quad (9)$$

where $I_F(k)$ and $I_F(k+1)$ are the link current of k'th and (k+1)'th switching cycle during freewheeling operation.

From the equation (9) it can be seen that the link current is controlled by the duration of Δt_4 and Δt_6. For the regenerative operation the link current can be similarly regulated.

Most of high frequency topologies based on resonant link concept achieve zero-voltage switching by taking the inverter input voltage to zero prior to turn-off or turn-on of the switches. However, this converter accomplishes it by turning-on or turning-off the bridge switches when the voltage of shunt capacitor becomes the reflected voltage to the link. To assure zero-voltage switching condition in all cases, the voltage swing of shunt capacitor exceeds maximum source voltage(V_S). By rewriting the equation (8.5)

$$v_{C2}(t_8)=\sqrt{v_{C2}(t_7)^2+(L_R/C_R)i_{Lr}(t_7)^2} \quad (8.5)$$

it is noted that the voltage peak of shunt capacitor can be controlled by $i_{Lr}(t_7)$, since $v_{C2}(t_7)$ is not controllable during commutation interval. Fig. 10 shows the normalized current $i_{Lr,N}$ required for the peak voltage αV_S as a function of the normalized link voltage $v_{C2,N}$ at time t_7 where (V_S/Z_r) and V_S are the normalization factor for the current and voltage. Considering the series resistance(R_S) of the link during Mode P1, the voltage equation of $v_{C1}(t)$ is expressed as follows:

$$v_{C1}(t)= e^{-\beta t}\frac{\alpha V_S}{2}(1-\cos\sqrt{2}\omega_D t) \quad (10)$$

where

$$\omega_D = \sqrt{\omega_r^2-\beta^2} \quad (11)$$

$$\omega_r = 1/\sqrt{L_R C_R}. \quad (12)$$

$$\beta=\frac{R_S}{2L_R}. \quad (13)$$

From the equation (10) the peak value of $v_{C1}(t)$ can be approximated as follows:

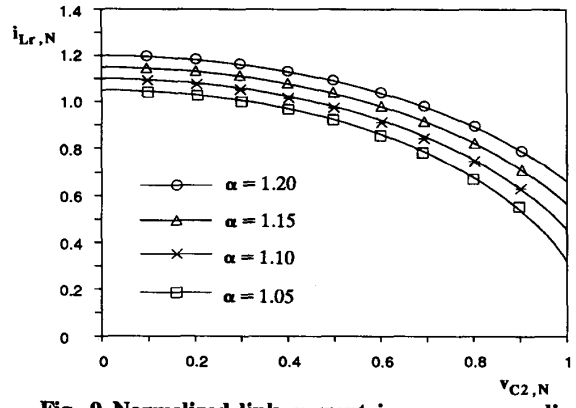

Fig. 9 Normalized link current $i_{Lr,N}$ vs. normalized voltage $v_{Cr,N}$ at time t_7 for several α

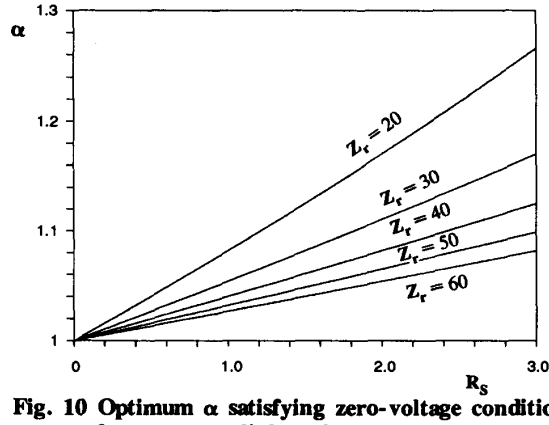

Fig. 10 Optimum α satisfying zero-voltage condition for non-zero link resistance

$$v_{C1,peak} = e^{-(\pi R_s)/(2Z_r)}\alpha V_S \quad (14)$$

Therefore, the condition for zero-voltage switching is given by

$$e^{-(\pi R_s)/(2Z_r)}\alpha \geq 1. \quad (15)$$

Since large α accompanies the augment of device voltage stress, minimum α is desired unless it violates the zero-voltage switching condition. Fig. 11 shows the optimum α satisfying the condition for zero-voltage switching.

V. SIMULATION RESULTS

The proposed converter is simulated to verify the operation. The current and voltage waveforms of the link operating at about 30kHz are shown in Fig. 12. The parameters used for simulations are as follows:

L_R = 30 μH

L_F = 1 mH

C_R = 30 nF

C_O = 30 μF.

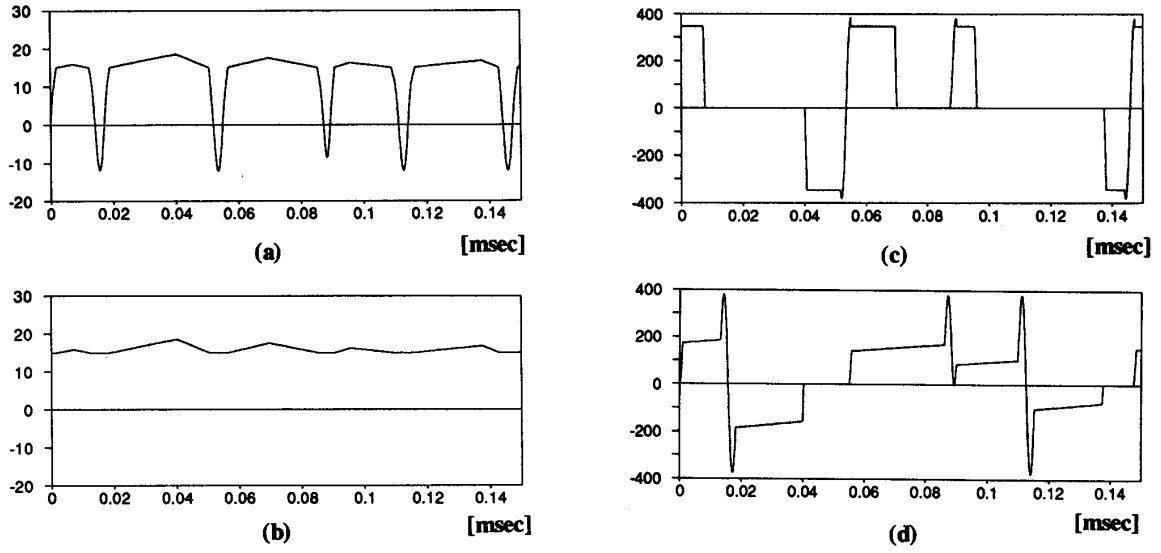

Fig. 11 Voltage and current waveforms of the link
(a) i_{Lr} (b) i_{Lf} (c)v_{C1} (d)v_{C2}

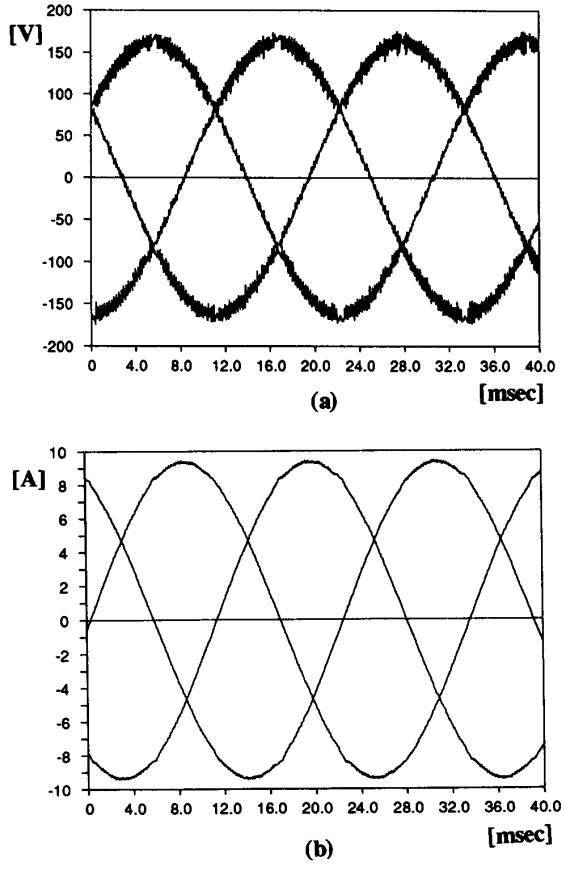

Fig. 12 Simulation results for 30Hz
(a) output line-line voltage
(b) load current

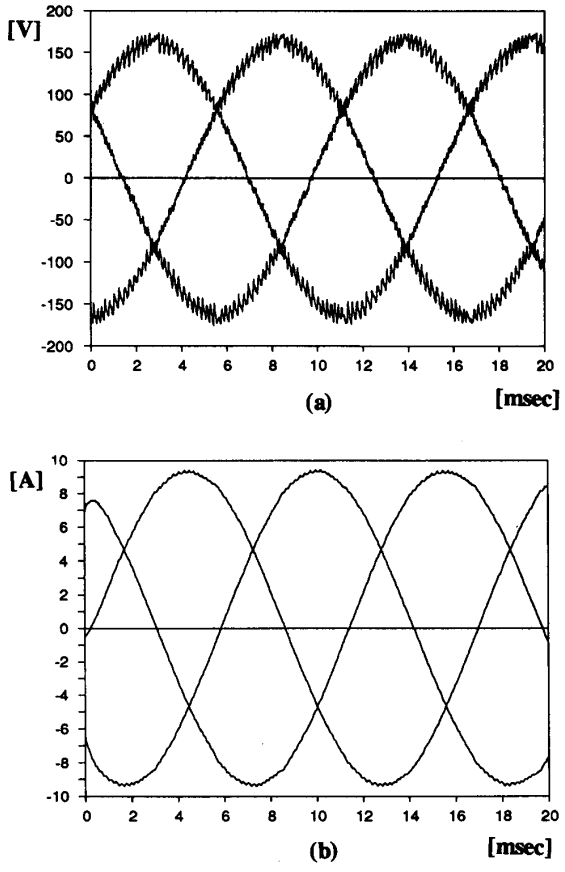

Fig. 13 Simulation results for 60Hz
(a) output line-line voltage
(b) load current

The voltage stresses of the reactive elements and the switches are determined by the voltage across two shunt capacitors. The simulation results show that the voltage stresses on all of the devices are almost equal to source voltage and the peak current stresses are limited to average link current. Fig. 13 and Fig. 14 show simulated waveforms of voltages and currents under steady-state operations at the frequency of 30Hz and 60Hz, respectively. It can be seen that the output voltage is well regulated.

VI. CONCLUSIONS

In this paper a new converter is proposed, which synthesizes sinusoidal voltage at the output terminals. All of the switchings occur at soft switching condition: inverter bridge switches under zero-voltage condition and the freewheeling switch under zero-current condition so that high frequency operation is possible due to the reduction of switching losses. The freewheeling switch provides the freewheeling path of the link current during the commutation interval, which separates the main power flow from the resonating circuit for zero-voltage switching condition. Therefore the voltage stresses can be controlled to be almost input source voltage, slightly increased for $\alpha > 1$ and the current peak on the link is limited to around average link current. Consequently the VA ratings of the elements which are extensively large to be serious in resonant link schemes are considerablely reduced in this converter. Not only this converter operates well on four quadrant but also it could operate on almost unity power factor.

REFERENCES

[1] B. O. Woo, I. D. Kim and G. H. Cho, "Zero voltage switching ac/dc/ac converter using modified high frequency dc-link" , *IEEE IAS Rec., pp. 1243-1250, 1990.*

[2] D. M. Divan, "Resonant dc link converter - a new concept in static power conversion", *IEEE IAS Rec., pp. 267-280, 1986.*

[3] D. M. Divan and G. Skibinski, "Zero-switching-loss inverter for high-power applications", *IEEE Trans. Ind. Appl., vol. 25; No. 4 pp. 634-643 Jul/Aug, 1989.*

[4] R. W. De Doncker and J. P. Lyons, "The auxiliary resonant commutated converter", *IEEE IAS Rec., pp. 1228-1235, 1990.*

[5] A. Cheriti, K. Al-Haddad, et al, "A rugged soft commutation PWM inverter for ac drives", *IEEE PESC Rec., pp. 656-662, 1990.*

[6] S. S. Park and G. H. Cho, " A current regulated pulse width modulation method with new series resonant inverter", *IEEE IAS Rec., pp. 1045-1051, 1989.*

[7] Y. Murai and T. A. Lipo, "High frequency series resonant dc-link power conversion", *IEEE IAS Rec., pp. 772-779, 1988.*

[8] Jih-Sheng Lai and B. K. Bose, "An improved resonant dc link inverter for induction motor drives", *IEEE IAS Rec., pp. 627-634, 1987.*

[9] Jih-Sheng Lai and B. K. Bose, "High frequency quasi-resonant dc voltage notching inverter for ac motor drives", *IEEE IAS Rec., pp. 1203-1217, 1990.*